Published in final edited form as:

J Biomol NMR. 2016 May ; 65(1): 41–48. doi:10.1007/s10858-016-0037-x.

Site specific polarization transfer from a hyperpolarized ligand of dihydrofolate reductase

Yunyi Wang[1], **Mukundan Ragavan**[1,2], and **Christian Hilty**[1]

[1] Chemistry Department, Texas A&M University, 3255 TAMU, College Station, TX 77843, USA

Abstract

Protein–ligand interaction is often characterized using polarization transfer by the intermolecular nuclear Overhauser effect (NOE). For such NOE experiments, hyperpolarization of nuclear spins presents the opportunity to increase the spin magnetization, which is transferred, by several orders of magnitude. Here, folic acid, a ligand of dihydrofolate reductase (DHFR), was hyperpolarized on ^{1}H spins using dissolution dynamic nuclear polarization (D-DNP). Mixing hyperpolarized ligand with protein resulted in observable increases in protein ^{1}H signal predominantly in the methyl group region of the spectra. Using ^{13}C single quantum selection in a series of one-dimensional spectra, the carbon chemical shift ranges of the corresponding methyl groups can be elucidated. Signals observed in these hyperpolarized spectra could be confirmed using 3D isotope filtered NOESY spectra, although the hyperpolarized spectra were obtained in single scans. By further correlating the signal intensities observed in the D-DNP experiments with the occurrence of short distances in the crystal structure of the protein–ligand complex, the observed methyl proton signals could be matched to the chemical shifts of six amino acids in the active site of DHFR-folic acid binary complex. These data demonstrate that ^{13}C chemical shift selection of protein resonances, combined with the intrinsic selectivity towards magnetization originating from the initially hyperpolarized spins, can be used for site specific characterization of protein–ligand interactions.

Keywords

Dissolution dynamic nuclear polarization; Nuclear magnetic resonance; Protein–ligand interaction; Drug discovery

Introduction

Observing spin polarization transfer based on the nuclear Overhauser effect (NOE) is one of the most direct ways to confirm the existence of an intermolecular interaction. Applied to proteins, NOE transfer allows the determination of protein–protein binding interfaces (Garrett et al. 1999; Zuiderweg 2002), as well as the identification of binding pockets for

Christian Hilty chilty@tamu.edu.

[2]Present Address: Department of Biochemistry and Molecular Biology, College of Medicine, University of Florida, Gainesville, FL 32611, USA

Electronic supplementary material The online version of this article (doi:10.1007/s10858-016-0037-x) contains supplementary material, which is available to authorized users.

protein–ligand interaction (Clore and Gronenborn 1983; Campbell and Sykes 1993). The NOE is typically manifested as a small fractional change in signal obtained from a nuclear spin after perturbation of the equilibrium Zeeman population of another, nearby spin. In the case of intermolecular interactions, the magnitude of the spin polarization transferred due to the NOE is further reduced if the binding sites on target molecules are only fractionally occupied. Consequently, observation of intermolecular NOEs can be subject to important sensitivity limitations. A powerful way of increasing NOE intensity, however, is through hyperpolarization. A hyperpolarized source spin exhibits a deviation from equilibrium spin polarization that is orders of magnitude larger than that of the simple population inversion achievable with the application of a radio-frequency pulse.

The spin polarization-induced nuclear Overhauser effect (SPINOE) from hyperpolarized xenon has been used to enhance signals of hydrophobic cavities in proteins (Landon et al. 2001). Surface accessibility of tryptophan residues furthermore can be studied in detail using chemically induced dynamic nuclear polarization, by a cyclic reaction with flavin (Kaptein et al. 1978). In this case, a change in solvent accessibility during protein folding has been found. Polarization transfer from molecules that are directly hyperpolarized on proton spins using dissolution dynamic nuclear polarization (Ardenkjær-Larsen et al. 2003) (D-DNP) is also possible. Ultrafast 2D NMR spectra of polarization transferred from water to exchangeable amide protons in proteins were reported (Olsen et al. 2016). In our previous work, we have demonstrated that polarization transfer from a specifically binding hyperpolarized ligand shows a spectrum similar to the frequency dependence of the transfer of saturation from the protein to the ligand (Min et al. 2015). Using D-DNP hyperpolarization, a two-step polarization transfer between competitively binding ligands, mediated by the protein, can be observed similar to the Interligand NOE for Pharmacophore Mapping (INPHARMA) experiment (Orts et al. 2009; Lee et al. 2012). While in the latter case the measured interligand NOE transfer rates are indicative of ligand orientation, additional structural information would be available from spectra of protein resonances, provided that they can be obtained with sufficient resolution.

Dihydrofolate reductase (DHFR) is an essential enzyme in both prokaryotes and eukaryotes, which reduces dihydrofolic acid (DHF) to tetrahydrofolic acid (THF) in the presence of the cofactor, dihydronicotinamide adenine dinucleotide phosphate (NADPH). Owing to its function of maintaining the cellular levels of THF and its derivatives, DHFR is an important enzyme involved in the folate cycle. This cycle produces precursors for purine and thymidylate synthesis. Hence, DHFR serves as a classic drug target and one of the most well studied enzymes (Schnell et al. 2004). Established antifolate drugs include antibacterial compounds trimethoprim (TMP) (Dauber-Osguthorpe et al. 1988) and the anticancer agent methotrexate (MTX) (Jolivet et al. 1983). While *Escherichia coli* (*E. coli*) DHFR has been most extensively studied, the amino acids required for catalysis and the general features of the secondary structures are conserved. For example, both the *E. coli* and the human protein have the binding site located at the junction of two subdomains (Abali et al. 2008; Liu et al. 2013). Structural characterization by X-ray crystal-lography (Matthews et al. 1977; Filman et al. 1982; Bystroff et al. 1990; Bystroff and Kraut 1991; Reyes et al. 1995; Sawaya and Kraut 1997) and NMR (Falzone et al. 1990, 1994) have revealed interactions of *E. coli* DHFR with various ligands.

Here, we used *E. coli* DHFR as a model protein to introduce a series of D-DNP NMR experiments that allow for the site specific resolution of NOE signals transferred from the ligand to the protein, by employing indirect selection based on ^{13}C chemical shift. We demonstrate selectivity by mapping side-chain resonances of the binding pocket of DHFR for the ligand folic acid, and discuss the utility of this method for obtaining limited structural information on the binding site.

Results and discussion

A ^{1}H NMR spectrum of hyperpolarized folic acid is shown in Fig. 1. When compared to the spectrum from a sample thermally polarized in the NMR magnet, all peaks for the ligands are enhanced significantly. The largest enhancement factors are 910 for H7, 700 for H2′/H6′, and 610 for H3′/H5′, while they vary between 100 and 200 for other folic acid peaks. For obtaining these spectra, a rapid injection system (Bowen and Hilty 2010) was used, allowing a sample transfer time of approximately 1200 ms. Polarization loss during the sample injection period was thereby minimized.

Due to the hyperpolarization of the ligand, polarization transfer to the protein leading to visible signals even in a single scan can be expected (Min et al. 2015). Enhanced signals in spectral regions characteristic of the protein, in particular side-chain protons, are indeed readily seen upon admixing of DHFR. Since these signals are not present in the sample of folic acid alone, and are not observable in a sample of protein without hyperpolarized ligand, it is apparent that these signals originate from nuclear Overhauser (NOE) transfer from the ligand to the protein. Although polarization transferred from a ligand to the protein specifically originates at the location of the binding site, the enhanced signals are expected to stem from a sufficiently large number of protons such that their individual identification is generally precluded using ^{1}H NMR alone.

In order to resolve overlapped protein ^{1}H peaks, one-dimensional spectra of the protein were acquired using a single-quantum filter for ^{13}C chemical shift selection. This pulse sequence, described in the Materials and Methods section, contains a selective refocusing pulse that can be adjusted for chemical shift position and selectivity. Spectra using filters with a full width at half maximum of 6900 and of 2100 Hz are shown in Fig. 2a, b, respectively. For comparison, a spectrum obtained with broad band ^{13}C filter is shown in Fig. 2c. This spectrum is expected to contain all of the protein signals that received sufficient NOE transfer from the hyperpolarized ligand. At the same time, the ^{13}C filter removes the coherences from unlabeled compounds and in this experiment ensures that the observed signals are from the protein. From the figure, it can be seen that the signals obtained with broad selection approximately represent the combination of the sets of signals observed in the individual traces. An increased selectivity with the narrower filter is further seen in the set of spectra in Fig. 2b, where fewer peaks are observed in each trace compared to the spectra in Fig. 2a. The frequency selection was achieved using Gaussian shaped pulses with the duration of 4000 or 7650 ms, in the case of the longer pulse also including simultaneous ^{1}H decoupling to prevent undesired effects due to *J*-coupling during the pulse time (Fig. 2d).

In order to relate observed chemical shifts to the structure, chemical shift assignments (Fig. S1 and S2) were mapped from Falzone et al. (1994), using triple resonance experiments to adjust for the sample conditions used as described in Materials and Methods. From the crystal structure of the complex (Sawaya and Kraut 1997), methyl protons located within 0.7 nm of one of the three ligand protons H7, H3′/H5′ or H2′/H6′ were further identified. Vertical lines at the chemical shift positions of these nearby methyl protons are drawn in Fig. 2a, b, and corresponding residue numbers are indicated at the top. Since the spectra acquired with selection at different ^{13}C chemical shifts show distinct patterns, it appears to be useful to map the observed peaks to the known ^{13}C and ^{1}H chemical shifts in the protein. For example, signal intensity at 0.32 ppm, which is near the proton resonance of Hδ1 for Ile50 (Hδ1: 0.32 ppm, Cδ1: 13.98 ppm), can be predominantly observed in the first spectra in Fig. 2a, b with selection pulse centered at 13.7 ppm. Furthermore, for almost every peak appearing in the DNP-NMR spectra between 0 and 1.5 ppm, a corresponding nearby protein proton within the selection range can be identified. In other words, there is a strong correlation between the observed signal intensities in the DNP-NMR spectra and the short ^{1}H–^{1}H distances identified from the X-ray crystal structure.

Protein–ligand NOEs can also be determined using conventional, non-hyperpolarized NMR spectroscopy—albeit not in a single scan, but rather in a multi-dimensional data set acquired over the course of several days. Specific intermolecular protein–ligand interactions can be investigated using isotope-filtered NMR methods (Otting and Wüthrich 1989; Breeze 2000), such as in a 3D ^{13}C-edited, $^{13}C/^{15}N$-filtered HSQC-NOESY spectrum using uniformly $^{13}C/^{15}N$-labeled protein combined with unlabeled ligand. Such a 3D HSQC-NOESY spectrum was measured with a mixing time of 500 ms. This spectrum contains exclusively intermolecular NOE peaks between the unlabeled folic acid and $^{13}C/^{15}N$-labeled DHFR with protein ^{13}C resonances in the ω_1 dimension, protein ^{1}H resonances in the ω_2 dimension and ligand ^{1}H resonances in the directly acquired ω_3 dimension.

NOE peaks between protein proton and different ligand protons can be obtained from analysis of the [ω_1/ω_2] planes at each folic acid ^{1}H chemical shift. Most of these cross peaks appear at the methyl group chemical shifts in the spectrum of the protein. These signals can be compared to the spectra obtained from the protein after NOE transfer from hyperpolarized ligand, which were acquired with a corresponding waiting time of 500 ms after admixing of the hyperpolarized ligand. The contact time in the DNP spectra is somewhat longer than 500 ms because of the sample mixing that occurs during part of the injection time. With the goal of comparing this 3D NOESY data with hyperpolarized spectra, it is necessary to consider the contribution of multiple ligand spins in both cases. Given that the signals from protons H7, H3′/H5′ and H2′/H6′ combined comprise 69 % of the total signal intensity of folic acid in the spectrum of Fig. 1a, the intensities in the planes of the 3D-NOESY spectrum corresponding to magnetization transferred to the ligand protons at three chemical shifts were added and shown in Fig. 2e (individual planes are shown in Fig. S3). No attempt was made to exactly scale the individual contributions since the integrals of these three signals vary in the 1D ^{1}H NMR spectrum of the hyperpolarized ligand. Differences arise due to different numbers of protons and other factors including differing polarization levels and varying polarization transfer efficiency.

The ^{13}C and ^{1}H chemical shift positions of the amino acid side chains in proximity to these protons are marked in Fig. 2e, with the corresponding residue number indicated. Almost all of the observed signal intensity in the spectrum is located at the positions identified using the distance ranges described above. In order to compare the DNP hyperpolarized spectra with the conventional NOESY spectrum, the regions corresponding to the full width at half maximum of the selection ranges in the DNP hyperpolarized spectra are further indicated in Fig. 2e. Almost all peaks shown in the DNP spectra in Fig. 2a, b can be correlated to the NOE peaks in the NOESY spectra, within the respective selection range. These results indicate that a series of DNP NOE experiments can provide intermolecular distance information with correlated ^{13}C chemical shift, similar to a 3D filtered HSQC-NOESY experiment.

The correlation of observed crosspeaks with the distances between protein and ligand ^{1}H can further be visualized by the structure shown in Fig. 3 (numerical distance values are listed in Table S1). The DNP-NMR spectra contain intensity at the chemical shift positions of the methyl groups of 6 amino acids; Ile5, Leu28, Thr35, Ile50, Leu54, Ile94. Their positions in the protein–ligand complex are all in the vicinity of the ligand molecule, as shown in the figure. For example, side chains of amino acid Ile50 (Hδ1: 0.32 ppm, Cδ1: 13.98 ppm; Hγ2: 0.52 ppm, Cγ2: 17.67 ppm) are in close contact with the (*p*-aminobenzoyl)-glutamate tail of folic acid. Hyperpolarization likely transferred from the highly polarized phenyl protons (H2′, H3′, H5′, H6′) yielded two strong peaks around 0.32 and 0.52 ppm (Fig. 2a, b). In Fig. 2b, where the selectivity in the ^{13}C dimension is increased, the former peak only appeared in the first spectrum (^{13}C selection at 13.7 ppm), whereas the latter can only be observed in the third spectrum with ^{13}C selection at 17.7 ppm. This difference is in accordance with the ^{13}C chemical shifts of the two methyl groups, which are 13.98 and 17.67 ppm, respectively. Based on this and other, similar observations made by comparing Fig. 2a, b with Fig. 3, it becomes apparent that structural information of protein–ligand complexes is available from the D-DNP experiments.

The hyperpolarized experiment with the ^{13}C single quantum filter is akin to a doubly selective conventional NMR experiment. In the DNP experiment, a first effective selection step is for the ligand, which is hyperpolarized to a level exceeding thermal polarization by a factor of at least 10^2–10^3. Since any NOE signals originating from the hyperpolarized ligand are amplified by this factor, many signals from non-polarized sample components—foremost the signals from the thermally polarized protein present at sub-millimolar concentration—can be neglected. A second selection step is represented by the spectroscopically applied filter, which primarily retains the signal of the ^{13}C enriched protein, with a selectivity of up to 1:99 based on the natural abundance of this isotope in unlabeled compounds. Therefore, the experiment becomes sensitive to the intermolecular NOE between the ligand and the protein alone. With the chemical shift selection, residue specific identification of intermolecular NOE becomes possible—a prerequisite for the use of such NOEs in applications requiring distance constraints. Additional selectivity may be achieved by other spectroscopic means, such as those based on *J*-coupling constants or on coupling multiplicity. The efficiency of recording an entire dataset with correlations may further be increased by Hadamard spectroscopy (Kupče et al. 2003), which we have in the past also applied with D-DNP (Chen and Hilty 2013), and similar correlations may also be

obtained using single-scan ultrafast 2D approaches (Frydman and Blazina 2007). The traditional 3D ^{13}C-edited, ^{13}C/^{15}N-filtered HSQC-NOESY experiments shown here was acquired over a time of 38 h, while one D-DNP experiment can be performed with a polarization step requiring less than 30 min, and almost instantaneous NMR acquisition. This rapid data acquisition in particular would lend itself to future applications to samples that show only a transient stability.

Conclusions

While traditional high-resolution NMR spectroscopy provides detailed structural information on biological macromolecules, these studies typically rely on multi-dimensional data sets that require acquisition times on the order of days. Applications that involve more rapid changes in the samples under study are often precluded. On the other hand, recent developments in hyperpolarization have demonstrated the potential of D-DNP for the study of fast processes by acquiring highly sensitive spectra of various nuclei. In the most basic implementation, D-DNP data however provide one-dimensional spectra that do not contain the resolution necessary for the identification of most individual resonances in biological macromolecules. Here, we demonstrate the combination of rapid acquisition using DNP-NMR, with an experiment providing structural information through [^{13}C, ^{1}H] single quantum selection in a protein of molecular weight of 18.8 kDa, which is too large for resolution of most individual peaks using homonuclear spectroscopy alone. This and other heteronuclear selection mechanisms provide a means for obtaining structural constraints in biomolecules using hyperpolarization by D-DNP.

Materials and methods

DHFR from *E. coli* was expressed from a plasmid pET-Duet-1 in *E. coli* BL21(DE3) cells. For unlabeled DHFR, cells were grown in LB medium and induced with 1 mM isopropyl β-D-1-thiogalactopyranoside (IPTG) at 37 °C. Uniformly ^{13}C/^{15}N-labeled DHFR was prepared using a protocol modified from Marley et al. (2001). Briefly, transformed cells were inoculated in 4 × 1 L LB medium and grown overnight at 37 °C and 250 rpm in an incubator shaker (Brunswick Instruments, New Brunswick, NJ) to an optical density of 0.6. Cells were centrifuged for 15 min at 5000×*g* and 4 °C, resuspended in 200 mL of M9 minimum medium (without glucose and ammonium chloride) and centrifuged again. The resuspension and centrifugation procedure was repeated a total of three times, in order to remove unlabeled growth medium components. Cells were subsequently resuspended in 1 L of M9 minimal medium containing 3 g of $^{13}C_6$-glucose and 1 g of ^{15}N-ammonium chloride and incubated at 37 °C and 250 rpm for 1 h. Protein expression was induced by addition of 1 mL of 1 M IPTG. After induction, cells were grown for an additional 20 h at 16 °C. Cells were harvested by centrifugation (5000×*g*, 15 min, 4 °C), resuspended in 50 mL of buffer A (20 mM sodium phosphate, 0.5 M NaCl, 5 mM imidazole, pH 7.4) and lysed by sonication on ice for 10 min. Cell lysate was centrifuged (10,000×*g*, 1 h, 4 °C), and the supernatant was loaded onto a 5 mL HisTrap HP column (GE Healthcare, Pittsburgh, PA). After washing with buffer A, the protein was eluted using buffer B (20 mM sodium phosphate, 0.5 M NaCl, 0.5 M imidazole, pH 7.4) with a linear gradient. Final purification was achieved by gel filtration using a Sephacryl S100 column (GE Healthcare) with 50 mM potassium

phosphate, 1 mM EDTA, 1 mM 1,4-dithiothreitol (DTT), 150 mM NaCl, pH 6.8. The purified protein was concentrated to 4.5 mM using a centrifugal filter device with 3 kDa molecular weight cutoff (EMD Millipore, Billerica, MA).

NMR spectroscopy was performed using a sample of 1.5 mM DHFR in 50 mM potassium phosphate, 1 mM EDTA, 1 mM DTT, 50 mM KCl, pH 6.8/10 % D_2O, with 15 mM folic acid, at a temperature of 298 K. Backbone and side chain chemical shift assignments were mapped from Falzone et al. (1994), using spectra acquired on a 500 MHz NMR spectrometer with a TCI cryoprobe (Bruker Biospin, Billerica, MA). The spectra for assignment were HNCO (128 × 48 × 1024 complex points in ^{13}C, ^{15}N and ^{1}H dimensions with $t_{1,max}$ = 31.8, 13.9 and 81.9 ms, respectively), HNCA (96 × 64 × 1024 complex points in ^{13}C, ^{15}N and ^{1}H dimensions with $t_{1,max}$ = 12.7, 19.7 and 81.9 ms, respectively), HNCACB (160 × 64 × 1024 complex points in ^{13}C, ^{15}N and ^{1}H dimensions with $t_{1,max}$ = 9.8, 18.6 and 81.9 ms, respectively), H(CC)(CO)NH-TOCSY (128 × 40 × 2048 complex points in ^{1}H, ^{15}N and ^{1}H dimensions with $t_{1,max}$ = 16.0, 12.3 and 163.8 ms, respectively, τ_m = 15 ms), (H)CC (CO)NH-TOCSY (170 × 44 × 1024 complex points in ^{13}C, ^{15}N and ^{1}H dimensions with $t_{1,max}$ = 10.2, 13.6 and 81.9 ms, respectively, τ_m = 15 ms), and HCCH-TOCSY (128 × 64 × 2048 complex points in ^{1}H, ^{13}C and ^{1}H dimensions with $t_{1,max}$ = 12.8, 3.4 and 163.8 ms, respectively, τ_m = 15 ms). NOEs between ligand and protein were identified from the same sample by acquiring a HSQC-NOESY (80 × 128 × 2048 complex points in ^{13}C, ^{1}H and ^{1}H dimensions with $t_{1,max}$ = 4.2, 9.8 and 157.7 ms, respectively, τ_m = 500 ms).

For hyperpolarized NMR, aliquots of 10 μL volume were prepared containing 225 mM folic acid and 15 mM 4-hydroxy-2,2,6,6-tetramethylpiperidin-1-oxyl (TEMPOL) in D_2O/DMSO-d6 (1:1 v/v). Aliquots were irradiated in a HyperSense DNP polarizer (Oxford Instruments, Abingdon, UK) at a microwave frequency of 94.005 GHz optimized for ^{1}H polarization, microwave power of 100 mW and temperature of 1.4 K. After 20 min, hyperpolarized samples were dissolved in 4 mL of 50 mM potassium phosphate, pH 6.8, which had been pre-heated in a closed vessel until a pressure of 1 MPa had been reached (time point a in Fig. 4). Dissolved samples were taken into the loop of a sample injector device (Bowen and Hilty 2010). A volume of 450 μL was injected into a 5 mm NMR tube, during 380 ms (starting from time point b, and finishing at time point c in Fig. 4) using nitrogen gas at a pressure of 1.81 MPa against a back pressure of 1.03 MPa. The empty NMR tube, or the NMR tube that had been loaded with 25 μL of 4.5 mM DHFR in 50 mM potassium phosphate, pH 6.8, had been pre-installed in a 400 MHz NMR spectrometer equipped with a broadband observe (BBO) probe (Bruker Biospin, Billerica, MA) set to a temperature of 298 K. In the case of the NMR tube loaded with DHFR, the hyperpolarized folic acid mixed with the protein during injection. In both cases, NMR spectroscopy was performed starting at time point d in Fig. 4, immediately following a delay of 500 ms after completion of injection.

^{1}H NMR spectra of hyperpolarized folic acid alone were acquired using a single $\pi/2$ pulse with water suppression by selective excitation. The same pulse sequence was used for acquiring spectra of DHFR in the presence of hyperpolarized folic acid, when not using isotope selection. NMR data with ^{13}C isotope selection were acquired using single quantum coherence transfer (Wagner and Berger 1997) (Fig. 4). For the refocusing pulse at the center

of the ^{13}C coherence evolution time, a Gaussian shape with 4000 or 7650 ms duration and 1 % truncation level was used for chemical shift selection, or a hard pulse with γB_1 = 27.8 kHz for broad band ^{13}C selection. GARP decoupling was applied on ^{13}C with γB_1 = 3.1 kHz during acquisition, WALTZ-16 decoupling on ^{1}H with γB_1 = 3.1 kHz can be turned on during the selective refocusing pulse for improved selectivity on ^{13}C. Spectra were processed with an exponential window function (25 Hz line broadening) and polynomial baseline correction using TopSpin 3.2 (Bruker Biospin).

Supplementary Material

Refer to Web version on PubMed Central for supplementary material.

Acknowledgments

We thank Dr. Wenshe Liu for providing the plasmid for expression of DHFR. Financial support from the National Institutes of Health (Grant R21-GM107927) and the Welch Foundation (Grant A-1658) are gratefully acknowledged.

Abbreviations

D-DNP	Dissolution dynamic nuclear polarization
DHF	Dihydrofolic acid
DHFR	Dihydrofolate reductase
INPHARMA	Interligand NOE for pharmacophore mapping
MTX	Methotrexate
NADPH	Dihydronicotinamide adenine dinucleotide phosphate
NOE	Nuclear Overhauser effect
NOESY	Nuclear Overhauser effect spectroscopy
SPINOE	Spin polarization-induced nuclear Overhauser effect
THF	Tetrahydrofolic acid
TMP	Trimethoprim

References

Abali EE, Skacel NE, Celikkaya H, Hsieh YC. Regulation of human dihydrofolate reductase activity and expression. Vitam Horm. 2008; 79:267–292. [PubMed: 18804698]

Ardenkjær-Larsen JH, Fridlund B, Gram A, Hansson G, Hansson L, Lerche MH, Servin R, Thaning M, Golman K. Increase in signal-to-noise ratio of>10,000 times in liquid-state NMR. Proc Natl Acad Sci USA. 2003; 100:10158–10163. [PubMed: 12930897]

Bowen S, Hilty C. Rapid sample injection for hyperpolarized NMR spectroscopy. Phys Chem Chem Phys. 2010; 12:5766–5770. [PubMed: 20442947]

Breeze AL. Isotope-filtered NMR methods for the study of biomolecular structure and interactions. Prog Nucl Magn Reson Spectrosc. 2000; 36:323–372.

Bystroff C, Kraut J. Crystal structure of unliganded *Escherichia coli* dihydrofolate reductase. Ligand-induced conformational changes and cooperativity in binding. Biochemistry. 1991; 30:2227–2239. [PubMed: 1998681]

Bystroff C, Oatley SJ, Kraut J. Crystal structures of *Escherichia coli* dihydrofolate reductase: the NADP ? holoenzyme and the folate-NADP + ternary complex. Substrate binding and a model for the transition state. Biochemistry. 1990; 29:3263–3277. [PubMed: 2185835]

Campbell AP, Sykes BD. The two-dimensional transferred nuclear Overhauser effect: theory and practice. Annu Rev Biophys Biomol Struct. 1993; 22:99–122. [PubMed: 8348000]

Chen H-Y, Hilty C. Hyperpolarized hadamard spectroscopy using flow NMR. Anal Chem. 2013; 85:7385–7390. [PubMed: 23834163]

Clore GM, Gronenborn AM. Theory of the time dependent transferred nuclear Overhauser effect: applications to structural analysis of ligand-protein complexes in solution. J Magn Reson. 1983; 53:423–442.

Dauber-Osguthorpe P, Roberts VA, Osguthorpe DJ, Wolff J, Genest M, Hagler AT. Structure and energetics of ligand binding to proteins: *Escherichia coli* dihydrofolate reductase-trimetho-prim, a drug-receptor system. Proteins Struct Funct Genet. 1988; 4:31–47. [PubMed: 3054871]

Falzone CJ, Benkovic SJ, Wright PE. Partial proton NMR assignments of the *Escherichia coli* dihydrofolate reductase complex with folate: evidence for a unique conformation of bound folate. Biochemistry. 1990; 29:9667–9677. [PubMed: 2271608]

Falzone CJ, Cavanagh J, Cowart M, Palmer AG, Mattews CR, Benkovic SJ, Wright PE. ^{1}H, ^{15}N and ^{13}C resonance assignments, secondary structure, and the conformation of substrate in the binary folate complex of *Escherichia coli* dihydrofolate reductase. J Biomol NMR. 1994; 4:349–366. [PubMed: 8019142]

Filman DJ, Bolin JT, Matthews DA, Kraut J. Crystal structures of *Escherichia coli* and Lactobacillus casei dihydrofolate reductase refined at 1.7 A resolution. II. Environment of bound NADPH and implications for catalysis. J Biol Chem. 1982; 257:13663–13672. [PubMed: 6815179]

Frydman L, Blazina D. Ultrafast two-dimensional nuclear magnetic resonance spectroscopy of hyperpolarized solutions. Nat Phys. 2007; 3:415–419.

Garrett DS, Seok YJ, Peterkofsky A, Gronenborn AM, Clore GM. Solution structure of the 40,000 Mr phosphoryl transfer complex between the N-terminal domain of enzyme I and HPr. Nat Struct Biol. 1999; 6:166–173. [PubMed: 10048929]

Jolivet J, Cowan KH, Curt GA, Clendeninn NJ, Chabner BA. The pharmacology and clinical use of methotrexate. N Engl J Med. 1983; 309:1094–1104. [PubMed: 6353235]

Kaptein R, Dijkstra K, Nicolay K. Laser photo-CIDNP as a surface probe for proteins in solution. Nature. 1978; 274:293–294. [PubMed: 683312]

Kupče E, Nishida T, Freeman R. Hadamard NMR spectroscopy. Prog Nucl Magn Reson Spectrosc. 2003; 42:95–122.

Landon C, Berthault P, Vovelle F, Desvaux H. Magnetization transfer from laser-polarized xenon to protons located in the hydrophobic cavity of the wheat nonspecific lipid transfer protein. Protein Sci. 2001; 10:762–770. [PubMed: 11274467]

Lee Y, Zeng H, Mazur A, Wegstroth M, Carlomagno T, Reese M, Lee D, Becker S, Griesinger C, Hilty C. Hyperpolarized binding pocket nuclear Overhauser effect for determination of competitive ligand binding. Angew Chem Int Ed. 2012; 51:5179–5182.

Liu CT, Hanoian P, French JB, Pringle TH, Hammes-Schiffer S, Benkovic SJ. Functional significance of evolving protein sequence in dihydrofolate reductase from bacteria to humans. Proc Natl Acad Sci USA. 2013; 110:10159–10164. [PubMed: 23733948]

Marley J, Lu M, Bracken C. A method for efficient isotopic labeling of recombinant proteins. J Biomol NMR. 2001; 20:71–75. [PubMed: 11430757]

Matthews DA, Alden RA, Bolin JT, Freer ST, Hamlin R, Xuong NH, Kraut J, Poe M, Williams M, Hoogsteen K. Dihydrofolate reductase: X-ray structure of the binary complex with methotrexate. Science. 1977; 197:452–455. [PubMed: 17920]

Min H, Sekar G, Hilty C. Polarization transfer from ligands hyperpolarized by dissolution dynamic nuclear polarization for screening in drug discovery. ChemMedChem. 2015; 10:1559–1563. [PubMed: 26315550]

Olsen G, Markhasin E, Szekely O, Bretschneider C, Frydman L. Optimizing water hyperpolarization and dissolution for sensitivity-enhanced 2D biomolecular NMR. J Magn Reson. 2016; 264:49–58. [PubMed: 26920830]

Orts J, Griesinger C, Carlomagno T. The INPHARMA technique for pharmacophore mapping: a theoretical guide to the method. J Magn Reson. 2009; 200:64–73. [PubMed: 19592283]

Otting G, Wüthrich K. Extended heteronuclear editing of 2D 1H NMR spectra of isotope-labeled proteins, using the $X(\omega_1, \omega_2)$ double half filter. J Magn Reson. 1989; 85:586–594.

Pettersen EF, Goddard TD, Huang CC, Couch GS, Greenblatt DM, Meng EC, Ferrin TE. UCSF Chimera—a visualization system for exploratory research and analysis. J Comput Chem. 2004; 25:1605–1612. [PubMed: 15264254]

Reyes VM, Sawaya MR, Brown KA, Kraut J. Isomorphous crystal structures of *Escherichia coli* dihydrofolate reductase complexed with folate, 5-deazafolate, and 5, 10-dideazatetrahydrofolate: mechanistic implications. Biochemistry. 1995; 34:2710–2723. [PubMed: 7873554]

Sawaya MR, Kraut J. Loop and subdomain movements in the mechanism of *Escherichia coli* dihydrofolate reductase: crystal-lographic evidence. Biochemistry. 1997; 36:586–603. [PubMed: 9012674]

Schnell JR, Dyson HJ, Wright PE. Structure, dynamics, and catalytic function of dihydrofolate reductase. Annu Rev Biophys Biomol Struct. 2004; 33:119–140. [PubMed: 15139807]

Wagner R, Berger S. A significant improvement of the gradient selected SELINCOR technique. Fresenius J Anal Chem. 1997; 357:470–472.

Zuiderweg ERP. Mapping protein–protein interactions in solution by NMR spectroscopy. Biochemistry. 2002; 41:1–7. [PubMed: 11771996]

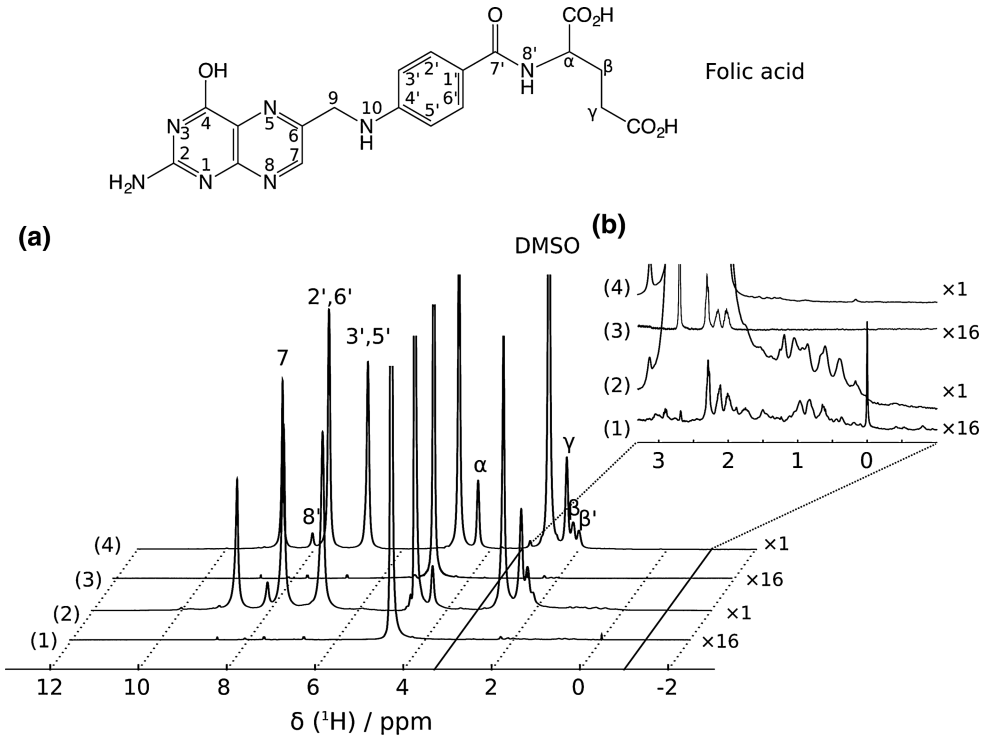

Fig. 1.

^{1}H NMR spectra **a** in full scale and **b** with aliphatic region enlarged to show enhanced protein peaks acquired with *1* thermally polarized folic acid with DHFR; *2* hyperpolarized folic acid mixed with preloaded DHFR; *3* thermally polarized folic acid without DHFR and *4* hyperpolarized folic acid without DHFR. Thermal spectra *1* and *3* are rescaled as 16 times of the original intensities

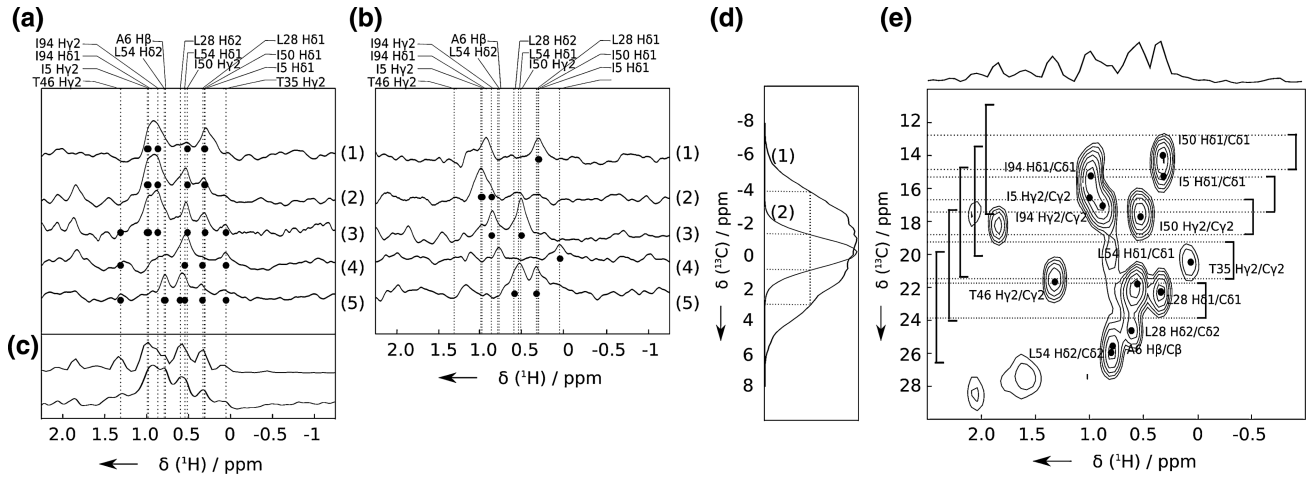

Fig. 2.

Comparison between DNP-NMR spectra and 3D filtered NOESY spectrum for observation of intermolecular NOE peaks between DHFR and folic acid. **a** DNP-NMR Spectra of DHFR in the presence of hyperpolarized folic acid, acquired with chemical shift selection at ^{13}C positions of *1* 13.7 ppm; *2* 16.2 ppm; *3* 17.7 ppm; *4* 20.2 ppm; *5* 22.7 ppm and width of 6900 Hz. *Dotted lines* represent the ^{1}H chemical shift of estimated NOE peaks based on ^{1}H–^{1}H distance (cutoff 0.7 nm) calculated from X-ray crystal structure (Sawaya and Kraut 1997), and *solid dots* indicate the estimated NOE peaks within the excitation region. **b** Spectra as in (**a**), but with selection width of 2100 Hz. **c** Comparison of spectra of DHFR in the presence of hyperpolarized folic acid, acquired with a hard excitation pulse (*bottom*) and 1D projection of the NOESY spectrum (*top*) from (**e**). **d** Experimentally determined excitation profiles of the pulse sequence used for selective excitation in the DNP-NMR experiments. **e** Superposition of three distinct ω_3 (ligand ^{1}H) planes (H7: 8.71 ppm, H2′/H6′: 7.65 ppm, H3′/H5′: 6.74 ppm) from the 3D HSQC-NOESY of ^{13}C,^{15}N-DHFR with unlabeled ligand. Estimated NOE peaks are calculated as in (**a**), and selection ranges are indicated. A 1D projection is shown at the *top*

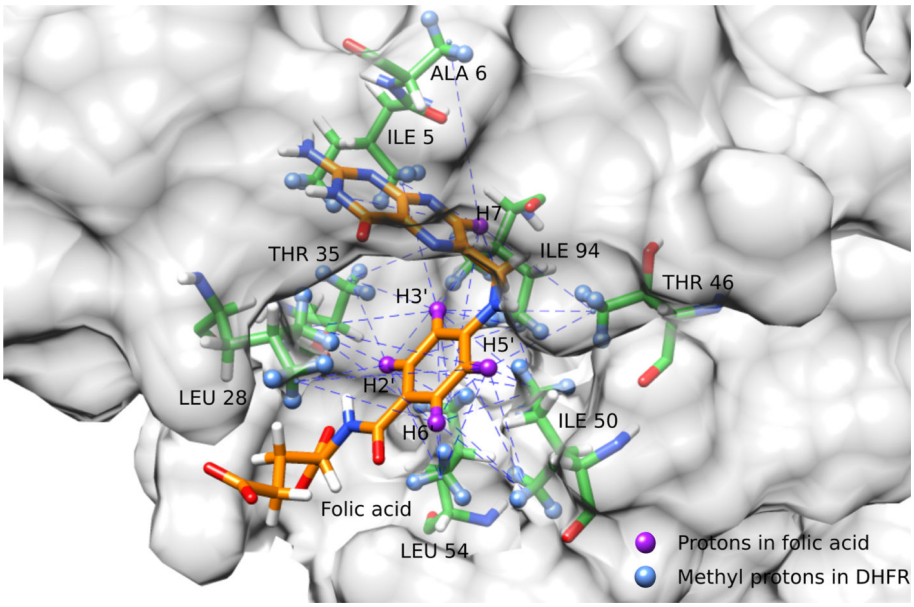

Fig. 3.

Crystal structure of folic acid-DHFR complex [Protein Data Bank 1RE7 (Sawaya and Kraut 1997), chain A]. Close distances (cutoff: 0.7 nm) between folic acid and DHFR methyl protons are indicated with *dashed lines*. H7, H2′, H3′, H6′, H7′ of folic acid are shown as *purple spheres*. *Blue spheres* indicate methyl protons in DHFR that are within 0.7 nm from the labeled folic acid protons. Image created with UCSF Chimera software version 1.10.2 (Pettersen et al. 2004)

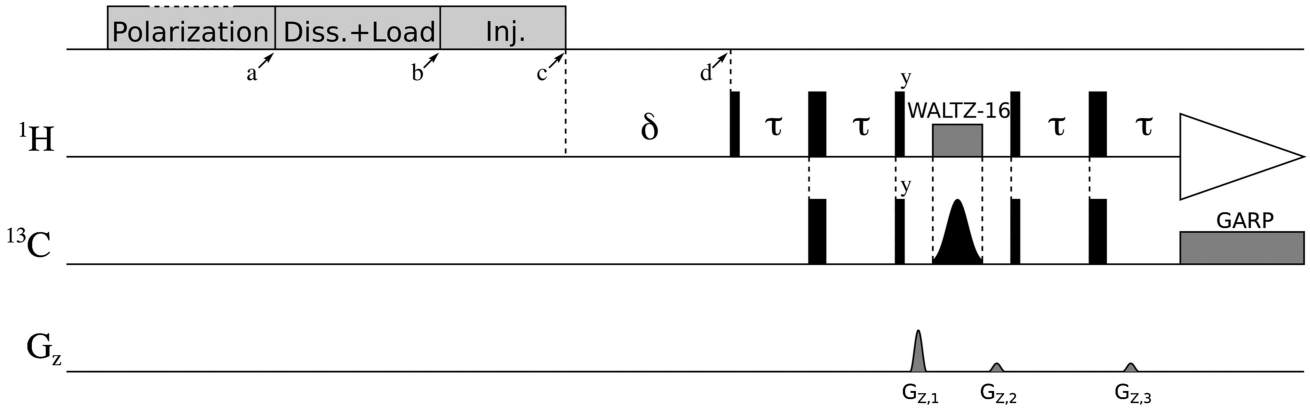

Fig. 4.

Experimental time line including sample polarization (20 min), dissolution ("diss."), loading into the injector loop, injection into the NMR instrument ("inj."; 380 ms), delay time δ = 500 ms and pulse sequence for DNP-NOE experiment. In the pulse sequence, narrow black bars represent **π**/2 pulses (γB_1 = 21.6 - kHz for ^{1}H, γB_1 = 27.8 kHz for ^{13}C). The pulse designated with a shape at the center of the ^{13}C coherence evolution time was applied either as a selective pulse for chemical shift selection, or as a hard **π** pulse for broad band ^{13}C selection (see text). Simultaneous proton decoupling during the selective carbon pulse can also be introduced by applying a WALTZ-16 pulse train (γB_1 = 3.1 kHz) (see text). GARP decoupling (γB_1 = 3.1 kHz) was applied on ^{13}C during acquisition. The delay was **τ** = 1.79 ms. Pulsed field gradients for coherence selection were $G_{z,1}$ = 32.1 G cm^{-1}, $G_{z,2}$ = 6.5 G cm^{-1} and $G_{z,3}$ = 6.5 G cm^{-1}